Ferromagnetism of V-doped ZnO nanowires*

Zhang Fu-Chun(张富春)†, Dong Jun-Tang(董军堂), Zhang Wei-Hu(张威虎), and Zhang Zhi-Yong(张志勇)

College of Physics and Electronic Information, Yan'an University, Yan'an 716000, *China*

(Received 1 April 2012; revised manuscript received 19 August 2012)

The geometry structures, electronic structures, and magnetic properties of $Zn_{46}V_2O_{48}$ nanowires are studied by density functional theory (DFT) calculations. We find that the ferromagnetic (FM) coupling is more stable for six configurations of $Zn_{46}V_2O_{48}$ nanowires, and is mediated by neighboring O as evidenced from the strong hybridization of V 3d and O 2p states, exhibiting strong spin polarization. The spin polarization is found to be 100% in the $Zn_{46}V_2O_{48}$ nanowires, which confirms that it is a half-metallic ferromagnet and very suitable for the injection of the spin carriers, which shows that $Zn_{46}V_2O_{48}$ nanowire is one of the ideal materials to realize spin electronic devices. At the same time, the magnetic coupling mechanisms of $Zn_{46}V_2O_{48}$ nanowires are analyzed with V 3d and O 2p orbitals and their magnetic moments mainly come from the contributions of the unpaired electrons of V 3d orbitals. The above results provide a theoretical basis for the preparation of 3d transition metal-doped ZnO nanowire materials.

Keywords: density functional theory, ZnO, nanowire, magnetism

PACS: 75.50.Pp, 71.55.Gs, 75.30.Hx **DOI:** 10.1088/1674-1056/22/2/027503

1. Introduction

Dilute magnetic semiconductors (DMSs) have attracted much attention because the electron charge and spin can be manipulated simultaneously, and have many unique potential applications in magneto–optical, magneto–electrical, and magneto–transport devices in the industrial application.[1–7] However, the DMSs based on II–VI group compound semiconductors such as CdTe and ZnSe only have the ferromagnetic (FM) properties of ultra-low Curie temperature or do not show FM properties; they do not have the value of application in the spin devices. As for the DMSs based on III–V group compound semiconductors (GaAs, InAs), the Curie temperature attained in the experiment only reaches about 200 K, far below the Curie temperature required by application ($T_C > 300$ K). In recent years, the research focus has gradually turned to the wide band gap semiconductors such as ZnO and GaN. In particular, DMSs based on ZnO have excellent electronic, magnetic, and optical properties. Moreover, for the 3d transition metals (TMs)-doped ZnO magnetic nanowires, because of the features of having a Curie temperature T_C above room temperature, large magnetic ion solubility, and being transparent in the range of visible light, the DMS is expected to become an important material in fields such as a new generation of information processing, storage, quantum computation, quantum communication, and spin devices, arousing much attention.[8–16] In addition, compared with the zero-dimensional material and film material, the 3d TMs-doped ZnO nanowire has a high blocking temperature and high magnetic coercivity, which has significant potential technological applications[17] in the preparation of nanodevices. Marcel *et al*.[18] studied the FM and AFM properties of (Zn, TMs)O (TMs=V, Cr, Mn, Fe, and Co) using first-principles calculation, and the calculation results showed that V, Ni, and Cu each have ferromagnetism, and Mn has anti-ferromagnetism, while Fe and Co have ferromagnetism and anti-ferromagnetism respectively. Xu *et al*.[19] synthesized V-doped ZnO nanorods by a low cost chemical approach, and the results showed an excellent high Curie temperature. Gupta and Kumar[20] reported on the observation of a high Curie temperature with a high remnant polarization and low coercive field in V-doped ZnO nanorods. Benjamin *et al*.[21] studied 3d TMs-doped ZnO nanowires. Yang *et al*.[22] reported on limited information about the FM behavior of V-doped ZnO. Hong[23,24] also observed room temperature ferromagnetism and a spin-glass-like behavior at low temperature; Venkatesan *et al*.[25] observed room temperature ferromagnetism in (110) oriented ZnO film. Ishida *et al*.[26] performed a soft X-ray magnetic circular diachronic study of a $Zn_{1-x}V_xO$ thin film and showed a small ferromagnetic moment. However, Ramachandran *et al*.[27] and Zhou *et al*.[28] did not observe any pronounced ferromagnetism exhibited by the V-doped ZnO at room temperature. To understand these conflicting results it is necessary for us to study the microscopic mechanism of ferromagnetic coupling for developing future applications of V-doped ZnO. In this work, we study systematically the structural and magnetic properties of V-doped ZnO nanowire, and reveal its magnetic coupling mechanism and origin of magnetism so as to provide the theoretical basis for the preparation of the high quality, and

*Project supported by the National Natural Science Foundation of China (Grant No. 60976069), the Natural Science Basic Research Plan in Shaanxi Province, China (Grant No. 2010JM8020), the Scientific Research Program of the Educational Committee of Shaanxi Province, China (Grant No. 11JK0846), and the Scientific Research Foundation of Yan'an University, China (Grant Nos. YDZD2011-03 and YD2010-01).

†Corresponding author. E-mail: zhangfuchun72@163.com

© 2013 Chinese Physical Society and IOP Publishing Ltd

high Curie temperature DMSs based on ZnO.

2. Theoretical models and calculated methods

2.1. Theoretical models

The calculation models for V-doped ZnO nanowires are based on wurtzite ZnO 7×7×2 supercell model (see Fig. 1(a)). First, we remove all atoms outside of the dotted line in Fig. 1(a) to build up the supercell structure of ZnO nanowires shown in Fig. 1(b): the supercell structure contains 96 atoms ($Zn_{48}O_{48}$). In order to reduce the influence of interaction between ZnO nanowires on the result, we assume that the vacuum space of ZnO nanowires along the directions of $[01\bar{1}0]$ and $[10\bar{1}0]$ is 10 Å (1 Å = 0.1 nm), while the ZnO nanowire along the direction of [0001] is of periodic structure. In order to study the magnetic coupling mechanism of V-doped ZnO nanowires, we adopt two V atoms to replace two Zn atoms in each of the ZnO nanowires, and the six possible magnetic coupling models are as shown in Fig. 2, where figure 2(f) is for the V atom to realize indirect magnetic coupling through the O atom in the interlayer, and the other models are for two V atoms to form internal magnetic coupling through the O atom. This corresponds to a V concentration of 4.2%.

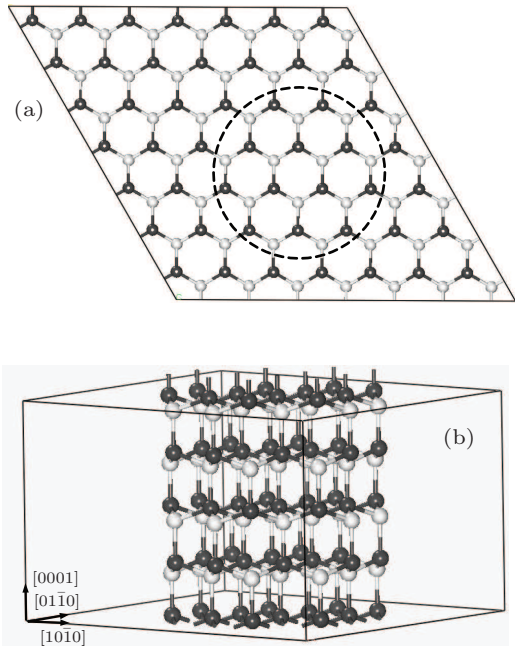


Fig. 1. (a) Top view of a 7×7×2 ZnO supercell with wurtzite structure, (b) $Zn_{48}O_{48}$ supercell which yields a nanowire along [0001] direction. (The white spheres denote O atoms, and the black spheres refer to Zn atoms).

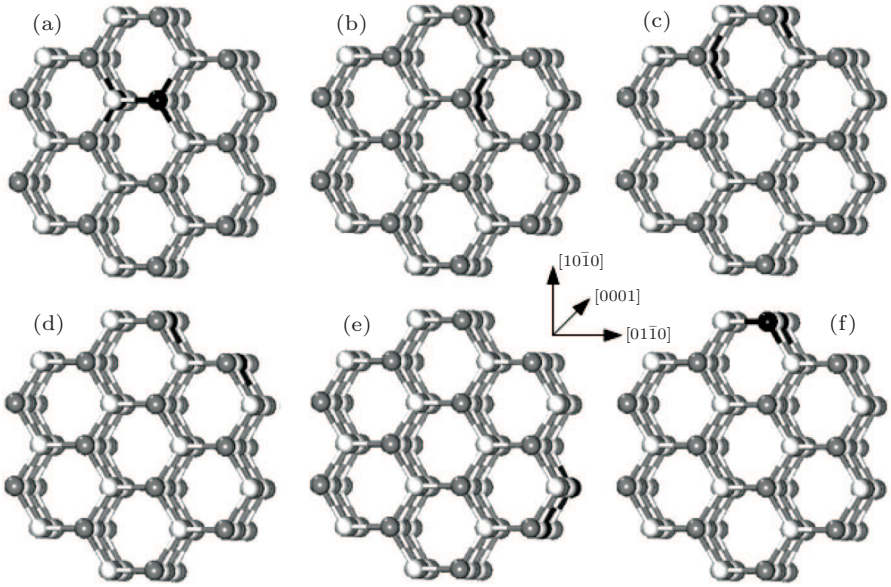


Fig. 2. Six configurations of V-doped ZnO nanowire magnetic coupling models (the black spheres denote V atoms, the white spheres represent O atoms, and the gray spheres refer to Zn atoms): (a) configuration I, (b) configuration II, (c) configuration III, (d) configuration IV, (e) configuration V, (f) configuration VI.

2.2. Calculation methods

The first-principles calculations are performed using the density-functional theory as implemented in the CASTEP package.[29] First, the V-doped ZnO nanowires are optimized in a geometric structure to obtain the stable $Zn_{46}V_2O_{48}$ nanowires. Second, the energy and basic properties of the optimized $Zn_{46}V_2O_{48}$ nanowires are calculated, and their attributes of FM and AFM of $Zn_{46}V_2O_{48}$ nanowires are also calculated. The ultra-soft pseudo potentials are used to describe the interaction potential between the ion core and valence electrons for Zn, O, and V, and Zn, O, and V valence electron configurations: $3d^{10}4s^2$, $3s^23p^4$, $3s^23p^63d^34s^2$ are selected. The

cutoff energy is set to be 420 eV and the residual forces on the atoms are less than 1 meV/Å. The internal stress is no more than 0.1 Gpa and a 1×1×16 Monkhorst–Pack K-point sampling is used for Brillouin zone integration.

3. Results and discussion

3.1. Geometric structures and stability analysis

In order to study V-doped ZnO nanowires, we also give geometric structures and electronic structures of $Zn_{48}O_{48}$ nanowires in relaxation. The calculated energy results show that the total energy of the relaxed $Zn_{48}O_{48}$ nanowire is 8.793 eV lower than the unrelaxed one, indicating that the relaxed ZnO nanowires are more stable. As for relaxed nanowires, the Zn–O bond length of the outermost layer along the direction of [0001] is 1.899 Å, which is shortened by 4.67% (1.992 Å), and the Zn–O bond lengths of the inner two layers are 1.978 Å and 1.969 Å, which are shortened by 0.7% and 1.15%, respectively. The Zn–O bond lengths of the outer layer along the direction of $[01\bar{1}0]$ is reduced from 1.962 Å to 1.955 Å, which are shortened by 1.75%, and the corresponding bond angles change from ∠O–Zn–O=∠Zn–O–Zn=108.04° to ∠O–Zn–O=113.76°, and ∠Zn–O–Zn=105.81°, but the relaxation of the bond lengths and bond angles between the inner layer atoms of ZnO nanowires are much smaller than those of the outer layer atoms. The above research results are consistent with ZnO surface results.[30] Figure 4(a) is the total density of states (DOS) of pure ZnO nanowire. It is observed from Fig. 4(a) that the total DOS curves for the spin-up and spin-down are identical, namely undoped ZnO nanowire is a non-magnetic material. But, compared with ZnO bulk, nanowires show surface states in a band gap, which are mainly caused by lower-dimensional ZnO nanowire quantum size and surface effects.

In Table 1 we also give the geometry parameters and the calculated results of $Zn_{46}V_2O_{48}$ nanowires, in which, the ΔE (ΔE_0) is the energy difference between the AFM sate and FM state of optimized $Zn_{46}V_2O_{48}$ (without optimization) and the $\Delta\varepsilon$ is the relative energy value obtained by comparing the energy values of 5 kinds of other configurations, with the ground state energy taken as the reference value. As shown in Table 1, the values of ΔE of six kinds of configurations are all positive, indicating that the FM states are more stable than the AFM states. In addition, the configurations II and III are relatively stable (0.000 eV and 0.012eV), the values of relative energy of the other four configurations are 0.037 eV (configuration IV), 0.043 eV (configuration I), 0.066 eV (configuration VI), 0.081 eV (configuration V), respectively. So configuration II corresponds to the ground state of $Zn_{46}V_2O_{48}$ nanowires, and its energy is 0.142 eV lower than AFM state energy. This is mainly because the impurity V atoms cause a release and reduction of the strain energy due to their closer atomic distance. At the same time, the calculated energy results show that they are much larger than the thermal energy k_BT (30 meV) and the $\Delta\varepsilon$ is very small, so it is easy for the $Zn_{46}V_2O_{48}$ nanowires to form room temperature FM materials, which is consistent with the experimental results.[18–21]

In addition, the magnetic moments of $Zn_{46}V_2O_{48}$ nanowires mainly come from the contributions of the unpaired electrons of V 3d orbitals. The magnetic moment differences between the two V atoms are 0.371 μ_B and 0.226 μ_B for configurations II and III, respectively. This is mainly due to the fact that the atomic distance between two V atoms is smaller than those in other configurations, and has a strong interaction between V1 atom and V2 atom. However, with the increase of the atomic distance between the V atoms, the magnetic coupling of the two V atoms is weakened, while the magnetic moments of the V atoms remain unchanged and the magnetic moment of the nearest neighbor O atom between the V1 atom and V2 atom begins to increase. Moreover, as the V–V bond length increases and the V–O bond length decreases the magnetic moments on the V atoms increase gradually, but the V–V distances are very different, which show that the V–O bond lengths have a great influence on determining the magnetic origin and magnetic coupling of the $Zn_{46}V_2O_{48}$ nanowires. In addition, from Table 1, the local magnetic moments on V atoms change from 2.223 μ_B to 0.336 μ_B, while the local magnetic moments on O atoms vary from −0.068 μ_B to 0.004 μ_B, so the total magnetic moment of $Zn_{46}V_2O_{48}$ nanowires is contributed to mainly by the 3d electrons of V^{2+}.

Table 1. Values of energy differences ΔE, ΔE_0, and relative energy $\Delta\varepsilon$ (in eV), bond lengths (in Å), and magnetic moments (in μ_B).

Configuration	ΔE/eV	ΔE_0/eV	$\Delta\varepsilon$/eV	Coupling	d_{V-O}/Å	d_{V-V}/Å	μ_{V1}/μ_B	μ_{V2}/μ_B	μ_O/μ_B
I	0.164	0.026	0.043	FM	1.864	3.242	1.800	1.777	–0.013
II	0.142	0.035	0.000	FM	1.870	2.485	0.765	0.394	–0.004
III	0.114	0.043	0.012	FM	1.882	2.458	0.562	0.336	0.005
IV	0.192	0.037	0.037	FM	1.859	2.886	1.401	1.403	–0.009
V	0.323	0.037	0.081	FM	1.764	2.903	2.021	2.034	–0.068
VI	0.369	0.028	0.066	FM	1.790	5.150	2.035	2.223	–0.039

3.2. Magnetic properties

In order to further understand the magnetic origin and magnetic coupling mechanism between 3d *TM*s atoms, we look at Fig. 3, which shows the V–V coupling mechanism in a crystalline field of a tetrahedron. The 3d states of V atoms in a crystalline field of a tetrahedron split into threefold degenerate t_{2g} states (d_{xy}, d_{yz},d_{xz}) and twofold degenerate e_g states ($d_{z^2-r^2}$, $d_{x^2-y^2}$), and the e_g states lie under t_{2g} states. However, V-doped ZnO nanowires each have a small crystal field splitting, namely their magnetic stabilities are determined by the partially occupied t_{2g} states but not by the e_g states. Therefore the major hybridizations occur between V 3d and O 2p orbitals, the bonding states t_{2g}^{b} appear in valence bands and the anti-bonding states t_{2g}^{a} occur in the bottom of conduction bands, while the local wave function of e_g state lies between the two states and the coupling is very weak, forming non-bonding states e_g^{e}. The above-mentioned properties can be clearly observed from the partial DOS of $Zn_{46}V_2O_{48}$ nanowires given in Fig. 4.

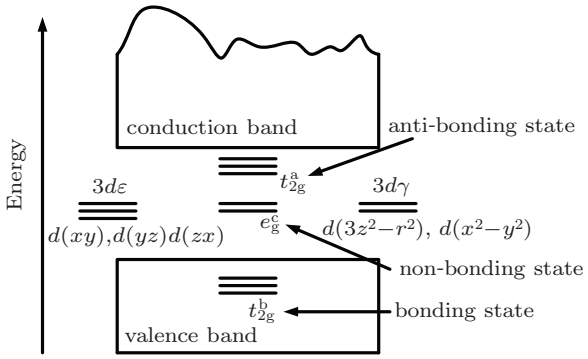


Fig. 3. Energy level diagram of V atom in a tetrahedral crystal field (T_d).

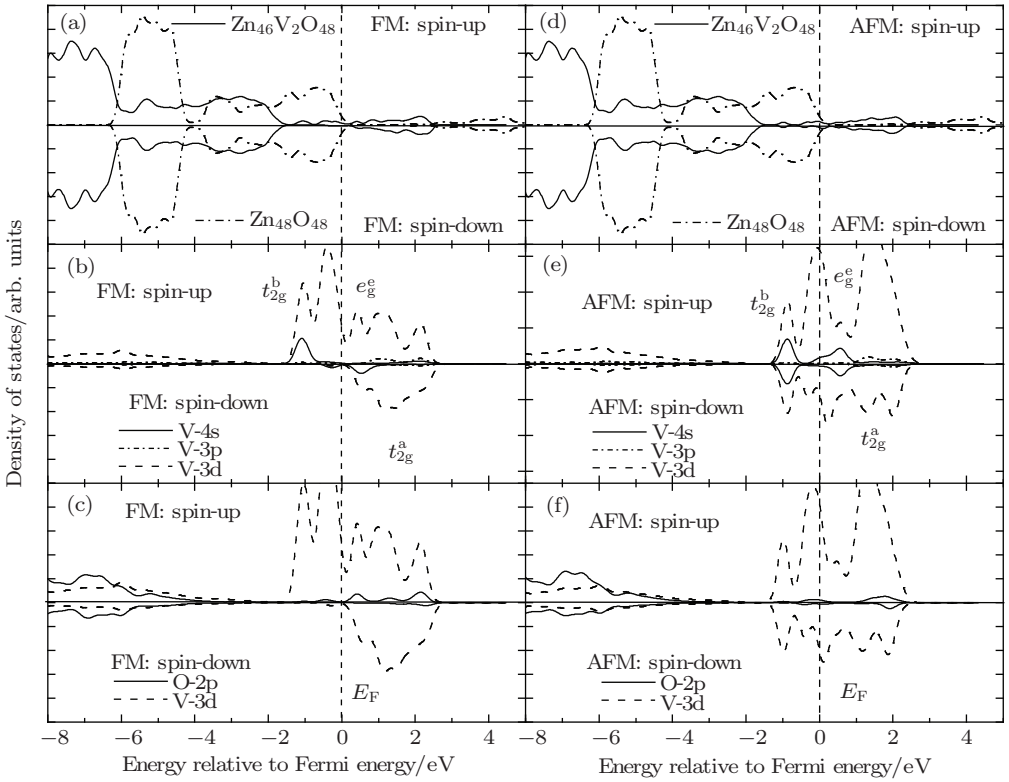


Fig. 4. Total DOSs and partial DOSs of $Zn_{46}V_2O_{48}$ nanowires.

As shown in Fig. 4, the lower valence bands (−8.0 V∼ −1.8 eV) are mainly contributed to by the O 2p and V 3d states, while the upper valence bands (−1.8 V∼ 0 eV) are mainly contributed to by the V 3d states. The conduction bands are mainly composed of V 3d and 4s states. Compared with the DOSs of V 3d states for the FM and AFM states, the spin-up energy levels extend much and the Fermi level passes through the gap for FM coupling, so the system is half-metallic and the materials are very suitable for the injection of spin carriers. At the same time, the V 3d state energy levels split into delocalized t_{2g} states and localized e_g states, and the p–d overlap at the valence bands can be observed between the t_{2g} and O 2p orbitals. So the $Zn_{46}V_2O_{48}$ nanowire has FM stability because the FM double-exchange interaction favors the filled V $3d^3$ states more than the AFM super-exchange interaction.[31] As can be seen from Figs. 4(b) and 4(c), due to the fact that there are the relatively large population of spin-up carriers and the large enough spin exchange splitting occur at the valence

bands, the electron spin is not reversed according to the first Hund's rule and therefore the FM states are stable. On the other hand, as shown in Figs. 4(e) and 4(f) of the AFM coupling, the DOSs of spin-up and spin-down distribute symmetrically, simply presenting weak spin splitting. Both spin-up and spin-down orbital levels extend through the Fermi level, thereby leading to a metallic behavior. Moreover, the DOS of AFM coupling moves in the high energy direction with respect to the FM coupling, and the anti-bonding states t_{2g}^{a} in the conduction band turn into being split, so the energy increases and the stability begins to decrease, which is consistent with the previous analyses of the stability and energy, indicating that $Zn_{46}V_2O_{48}$ nanowires more readily form FM coupling. These magnetic properties will be beneficial to exploiting more attractive electron spin devices with new functionality in ZnO-based DMS.

4. Conclusions

In the present study, the magnetic properties of the different magnetic coupling models of $Zn_{46}V_2O_{48}$ nanowires are calculated with spin-polarized density-functional theory. The coupling mechanisms of FM and AFM of the $Zn_{46}V_2O_{48}$ nanowires are compared and analyzed. The results show that $Zn_{46}V_2O_{48}$ nanowires have FM coupling features and the FM in the ground state is more stable. The strong p–d hybridization effect between V 3d and O 2p occurs at the valence band, which induces strong ferromagnetic interaction in $Zn_{46}V_2O_{48}$ nanowires. For the AFM coupling, the DOSs of the spin-up and spin-down orbitals distribute symmetrically and small spin splitting occurs only near the Fermi energy, and they are broadened and pass through the Fermi energy, showing a metallic behavior. In addition, the magnetic moments of $Zn_{46}V_2O_{48}$ nanowires mainly come from the contributions of the V 3d state electrons and part of the O 2p state electrons.

References

[1] Prinz G 1998 *Science* **282** 1600
[2] Ball P 2000 *Nature* **404** 918
[3] Wolf S A, Awschalom D D, Buhrman R A, Daughton J M, Molnár S, Roukes M L, Chtchelkanova A Y and Treger D M 2001 *Science* **294** 1488
[4] Young W S, Marvin L C and Steven G L 2006 *Nature* **444** 347
[5] Zhao L, Lu P F, Yu Z Y, Ma S J, Ding L and Liu J T 2012 *Chin. Phys.* B, **21** 097103
[6] Zhang X M, Zhang Y and Wang Z L 2008 *Appl. Phys. Lett.* **92** 162102
[7] Lin W X, Weng Z Z, Zhang J M and Huang Z G 2011 *Chin. Phys.* B **20** 027103
[8] Lu Z L, Zou W Q, Xu M X and Zhang F M 2010 *Chin. Phys.* B **19** 056101
[9] Xu Q Y, Wen Z, Gao J L, Wu D, Qiu T, Tang S L and Xu M X 2011 *Chin. Phys.* B **20** 087505
[10] Tara D, Devajyoti M, Robert H, Hariharan S, Pritish M and Sarath W 2010 *Mater. Res. Soc. Symp. Proc.* **1199** F03 44
[11] Dietl T, Ohno H, Matsukura F, Cibert J and Ferrand D 2000 *Science* **287** 1019
[12] Xu X G, Yang H L, Wu Y, Zhang D L and Jiang Y 2012 *Chin. Phys.* B **21** 047504
[13] He J H, Lao C S, Chen L J, Davidovic D and Wang Z L 2005 *J. Am. Chem. Soc.* **127** 16376
[14] Ul Haq B, Afaq A, Ahmed R and Naseem S 2012 *Chin. Phys.* B **21** 097101
[15] Cheng C W, Xu G Y, Zhang H Q and Luo Y 2008 *Mater. Lett.* **62** 1617
[16] Liao D Q, Shi E W, Chen Z Z and Zhou K J 2011 *Chin. Phys.* B **20** 037501
[17] Jun Y, Jung Y and Cheon J 2002 *J. Am. Chem. Soc.* **124** 615
[18] Marcel H F S, Kawazoe Y, Sharma P, Inoue A, Raju A R, Rout C and Waghmare U V 2005 *Phys. Rev. Lett.* **94** 187204
[19] Xu C K, Yang K K, Wang L W, Liu Y Y and Wang H 2008 *J. Phys.* D: *Appl. Phys.* **41** 195005
[20] Gupta M K and Kumar B 2011 *J. Mater. Chem.* **10** 1039
[21] Benjamin D Y, David O Z, Peter J P, Rongrui H and Peidong Y 2006 *Angew. Chem. Int. Ed.* **45** 420
[22] Yang Y C, Song C, Wang X H, Zeng F and Pan F 2008 *Appl. Phys. Lett.* **92** 012907
[23] Hong N, Sakai J and Hassini A 2005 *J. Appl. Phys.* **97** 103312
[24] Hong N, Sakai J and Hassini A 2005 *J. Phys.: Condens. Matter* **17** 199
[25] Venkatesan M, Fitzgerald C B, Lunney J G and Coey J M D 2004 *Phys. Rev. Lett.* **93** 177206
[26] Ishida Y, Hwang J I, Kobayashi M, Takeda Y, Mamiya K, Okamoto J, Fujimori S I, Okane T, Terai T K, Saitoh Y, Muramatsu Y, Fujimori A, Tanaka A, Saeki H, Kawai T and Tabata H 2007 *Appl. Phys. Lett.* **90** 022510
[27] Ramachandran S, Tiwari A, Narayan J and Prater J T 2005 *Appl. Phys. Lett.* **87** 172502
[28] Zhou S Q, Potzger K, Reuther H, Kuepper K, Skorupa W, Helm M and Fassbender J 2007 *J. Appl. Phys.* **101** 09H109
[29] Clark S J, Segall M D, Pickard C J, Hasnip P J, Probert M I J, Refson K and Payne M C 2005 *Z. Kristallogr.* **220** 567
[30] Wander A and Harrison N M 2000 *Surf. Sci. Lett.* **23** L342
[31] Akai H 1998 *Phys. Rev. Lett.* **81** 3002